

University of Wisconsin - Madison

MAD/PH/823

March 1994

THE INDIRECT DETECTION OF HALO DARK MATTER

F. HALZEN* and J. E. JACOBSEN

Dept. of Physics, University of Wisconsin, Madison WI 53706

Abstract

High energy particles are produced by the annihilation of dark matter particles in our galaxy. These are presently searched for using balloon-borne antiproton and positron detectors and large area, deep underground neutrino telescopes. Dark matter particles, trapped inside the sun, are an abundant source of such neutrinos.

From both the cosmological and particle physics points of view the lightest, stable supersymmetric particle or neutralino is arguably the leading dark matter candidate. Its mass is bracketed by a minimum value of order a few tens of GeV, determined from unsuccessful accelerator searches, and a maximum value of order 1 TeV imposed by particle physics as well as cosmological constraints. Back-of-the-envelope calculations are sufficient to demonstrate how present neutrino telescopes are competitive with existing and future particle colliders such as the LHC in the search for supersymmetry. We emphasize that a 1 km² area is the natural scale for a future instrument capable of probing the full GeV–TeV neutralino mass range by searching for high energy neutrinos produced by their annihilation in the sun.

1. Introduction

It is believed that most of our Universe is made of cold dark matter particles. Big bang cosmology implies that these particles have interactions of order the weak scale, i.e. they are WIMPS.¹ When our galaxy was formed the cold dark matter inevitably clustered with the luminous matter to form a sizeable fraction of the

$$\rho_\chi = 0.4 \text{ GeV/cm}^3 \quad (1)$$

galactic matter density implied by observed rotation curves. Unlike the baryons, the dissipationless WIMPS fill the galactic halo which is believed to be an isothermal sphere of WIMPS with average velocity

$$v_\chi = 300 \text{ km/sec.} \quad (2)$$

*Talk given at the *International Conference on Critique of the Sources of Dark Matter in the Universe*, UCLA, Los Angeles (1994)

Particle physics provides us with rather compelling candidates for WIMPS. The Standard Model is not a model. A most elegant and economical way to revamp it into a consistent and calculable framework is to make the model supersymmetric. If supersymmetry is indeed Nature's extension of the Standard Model it must produce new phenomena at or below the TeV scale. A very attractive feature of supersymmetry is that it provides cosmology with a natural dark matter candidate in form of a stable lightest supersymmetric particle.¹ There are a priori six candidates: the (s)neutrino, axi(o)n(o), gravitino and neutralino. They are, in fact, the only candidates because supersymmetry completes the Standard Model all the way to the GUT scale where its forces apparently unify. Therefore because supersymmetry logically completes the Standard Model with no other new physics threshold up to the GUT-scale, it must supply the dark matter. So, if supersymmetry, dark matter and accelerator detectors are on a level playing field. Here we will focus on the neutralino which, along with the axion, is for various reasons the most palatable candidate.² The supersymmetric partners of the photon, neutral weak boson and the two Higgs particles form four neutral states, the lightest of which is the stable neutralino

$$\chi = z_{11}\tilde{W}_3 + z_{12}\tilde{B} + z_{13}\tilde{H}_1 + z_{14}\tilde{H}_2. \quad (3)$$

In the minimal supersymmetric model (MSSM)³ down- and up-quarks acquire mass by coupling to different Higgs particles, usually denoted by H_1 and H_2 , the lightest of which is required to have a mass of order the Z -mass. Although the MSSM provides us with a definite calculational framework, its parameters are many. For the present discussion we only have to focus on the following terms in the MSSM lagrangian

$$L = \cdots \mu \tilde{H}_1 \tilde{H}_2 - \frac{1}{2} M_1 \tilde{B} \tilde{B} - \frac{1}{2} M_2 \tilde{W}_3 \tilde{W}_3 - \frac{1}{\sqrt{2}} g v_1 \tilde{H}_1 \tilde{W}_3 - \frac{1}{\sqrt{2}} g v_2 \tilde{H}_2 \tilde{W}_3 + \cdots, \quad (4)$$

which introduce the (unphysical) masses M_1 , M_2 and μ associated with the neutral gauge bosons and Higgs particles, respectively. M_1 and M_2 are related by the Weinberg angle. The lagrangian introduces two Higgs vacuum expectation values $v_{1,2}$; the coupling g is the known Standard Model SU(2) coupling. Although the parameter space of the MSSM is more complex, a first discussion of dark matter uses just 3 parameters

$$\mu, M_2, \text{ and } \tan \beta = v_2/v_1. \quad (5)$$

Further parameters which can also be varied include the masses of top, Higgs, squarks, etc.

Neutralino masses less than a few tens of GeV have been excluded by unsuccessful collider searches. For supersymmetry to resolve the fine-tuning problems of the Standard Model the masses of supersymmetric particles must be of order the weak scale and therefore, in practice, at the TeV scale or below. Also, if neutralinos have masses of order a few TeV and above, they overclose the Universe. Despite its rich parameter

space supersymmetry has therefore been framed inside a well defined GeV–TeV mass window with

$$\text{tens of GeV} < m_\chi < \text{TeV}. \quad (6)$$

Particles produced by the annihilation of WIMPS represent the experimental signature for the presence of halo dark matter. For the present discussion it is sufficient to focus on the dominant annihilation channels⁴

$$\chi + \bar{\chi} \rightarrow b + \bar{b} \quad (7)$$

or, if the WIMPS are sufficiently massive,

$$\chi + \bar{\chi} \rightarrow W^+ + W^- \quad (8)$$

2. Balloon-borne experiments

NASA runs a vigorous program of measurements of cosmic antiproton and positron fluxes using balloon-borne particle detectors operating near the top of the Earth's atmosphere.⁵ The instruments typically consist of a magnet, tracking and calorimetry which can separate electrons and protons. Such experiments provide us with an excellent opportunity to discover halo dark matter. Two possibilities are illustrated in Fig. 1. The b -quarks from halo dark matter annihilation hadronize into jets in ways that have been studied in much detail in accelerator experiments. Among the b -quark's hadronization products are low energy antiprotons which can be detected by balloon-borne antimatter detectors.⁶ Presence of dark matter is signaled by an excess \bar{p}/p flux in the sub-GeV region where the background is conveniently small. The origin of the background is the production of antiprotons in the interactions of cosmic rays with matter in the galaxy, e.g. the hydrogen in the disk. (The additional background of \bar{p} 's, produced in interactions of cosmic rays in the residual atmosphere above the balloon, can be calculated and subtracted.)

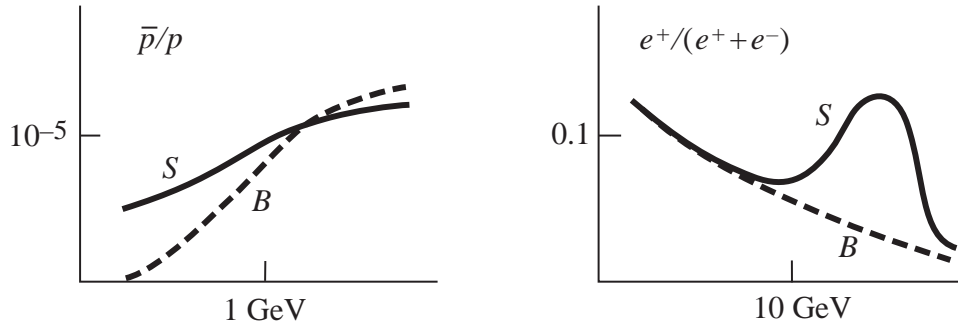


Fig. 1

An excess of positrons over and above the positron flux produced by the propagation of cosmic rays in the galaxy may also be a signature of dark matter. Semi-leptonic

decay of heavy quarks is the dominant contribution to the signal unless the neutralino mass is above threshold for annihilation into W 's. In this case the purely leptonic decay of the $W \rightarrow e^+ + \nu_e$ produces a “positron line” associated with the 2-body decay.⁷ In reality this “line” is broadened by the motion of the weak bosons into a high energy feature as sketched in Fig. 1.

The antiproton and positron flux of WIMP origin is proportional to the square of their halo density (1) and to their confinement time in the halo. The latter is unfortunately uncertain by roughly four orders of magnitude. Due to such astrophysical uncertainties the detection of WIMPS in these experiments can be by no means guaranteed. No exclusion limits can be derived from negative experiments. As we will see further on, this is in contrast with searches using the sun and Earth rather than the halo as the source of WIMPS. The low energy antiproton and high energy positron signatures are nevertheless virtually a “smoking gun” for particle dark matter in the halo and thus very much worthy of note.

3. Neutrino Signature of WIMP-Annihilation in the Sun

WIMPS, scattering off protons in the sun, loose energy. They may fall below escape velocity and be gravitationally trapped. Trapped dark matter particles eventually come to equilibrium temperature, and therefore to rest at the center of the sun. While the neutralino density builds up, their annihilation rate increases until equilibrium is achieved where the annihilation rate equals half of the capture rate. The sun has thus become a reservoir of neutralinos which annihilate into any open fermion, gauge boson or Higgs channels. The leptonic decays from annihilation channels such as $b\bar{b}$ and W^+W^- turn the sun into a source of high energy neutrinos. Their energies are in the GeV to TeV range, rather than in the familiar KeV to MeV range from its nuclear burning. These neutrinos can be detected in deep underground experiments. Figure 2 shows a cartoon of the chain of events leading from dark matter in the halo to a muon track, pointing back to the sun, in the Earth-based Cherenkov detector.

We will illustrate the power of neutrino telescopes as dark matter detectors using as an example the search for a 500 GeV neutralino, a mass outside the reach of present accelerator and future LHC experiments. It is a reasonable choice given that there are arguments, mostly related to fine-tuning of unruly radiative corrections in the Higgs sector of the Standard Model, that the mass of the neutralino should be well below 1 TeV.

No long and complex code is necessary to qualitatively evaluate the potential of high energy neutrino telescopes as dark matter detectors. For quantitative calculations such code exists and can be distributed to anyone interested.⁸

A calculation of the rate of high energy muons of neutralino origin triggering a detector is calculated in 5 easy steps.

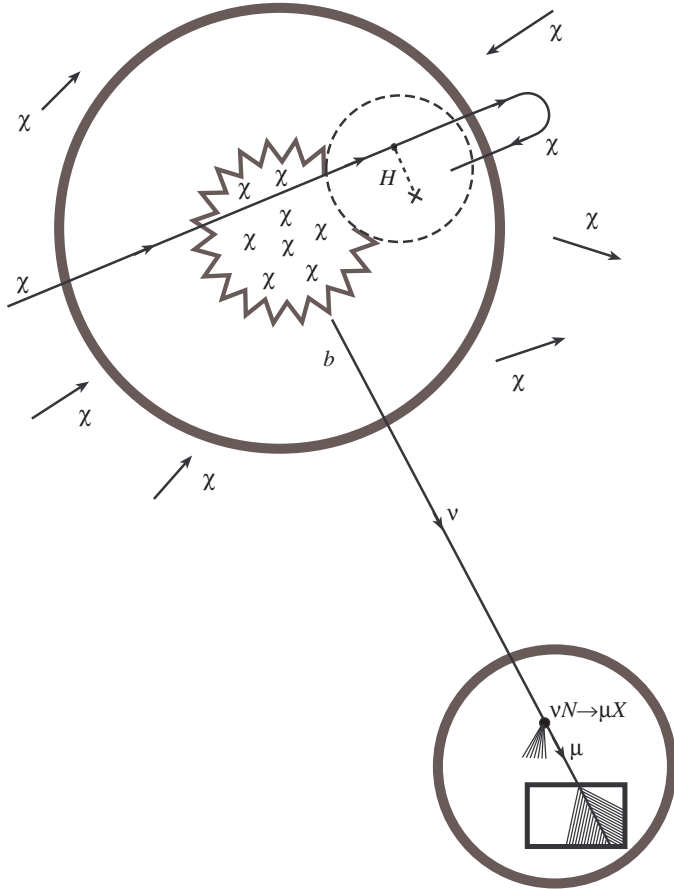


Fig. 2

Step 1: the halo neutralino flux ϕ_χ

It is given by their number density and average velocity of (1), (2). From (1)

$$n_\chi = 8 \times 10^{-4} \left[\frac{500 \text{ GeV}}{m_\chi} \right] \text{ cm}^{-3} \quad (9)$$

and therefore

$$\phi_\chi = n_\chi v_\chi = 2 \times 10^4 \left[\frac{500 \text{ GeV}}{m_\chi} \right] \text{ cm}^{-2} \text{ s}^{-1}. \quad (10)$$

Step 2: cross section σ_{sun} for the capture of neutralinos by the sun

The probability that a neutralino is captured is proportional to the number of target hydrogen nuclei in the sun (i.e. the solar mass divided by the nucleon mass) and the neutralino-nucleon scattering cross section. $\sigma(\chi N)$ receives contributions from 2 classes of diagrams: the exchange of Higgses and weak bosons, and the exchange of squarks; see Fig. 3. The result is often dominated by the large coherent cross section

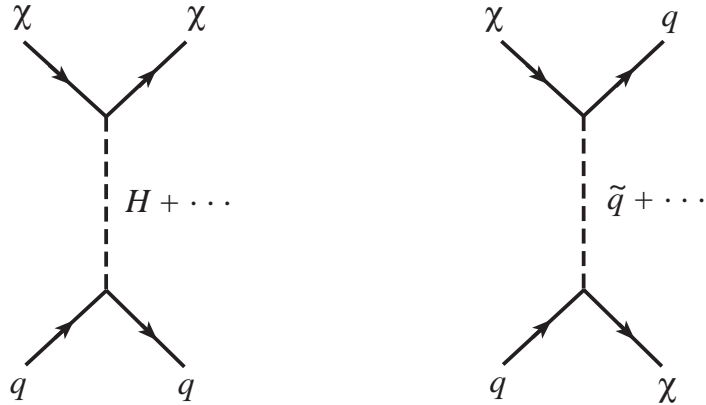


Fig. 3

associated with the exchange of the lightest Higgs particle H_2 and is of the form

$$\sigma = \alpha_H (G_F m_N^2)^2 \frac{m_\chi^2}{(m_N + m_\chi)^2} \frac{m_Z^2}{m_H^4} \quad (11)$$

or, for large m_χ

$$\sigma = \alpha_H (G_F m_N^2)^2 \frac{m_Z^2}{m_H^4}. \quad (12)$$

The proportionality parameter α_H is of order unity, but can become as small as 10^{-2} in some regions of the MSSM parameter space. This is illustrated in Fig. 4 where the MSSM parameter space is parametrized in terms of the unphysical masses $M(\mu)$ of the unmixed wino(Higgsino). (The ratio of the vacuum expectation values associated with the two Higgs particles $v_2/v_1 = 2$ is here fixed to some arbitrary value.) The relation of these parameters to the neutralino mass is shown in the figure. The full lines show fixed values of the neutralino mass m_χ . The lines labelled by squares trace fixed values of the “coupling” α_H . The dashed area indicates M, μ values which are excluded by cosmological considerations. In standard big bang cosmology neutralinos with the corresponding parameters will overclose the Universe. Note that for a given χ mass there are two possible states with the same α_H value. One of them will preferentially annihilate into weak bosons, the other into fermions. Therefore, their neutrino signature is provided by W, Z decay and semi-leptonic heavy quark decays, respectively. Figure 4 illustrates that for heavy neutralinos, which can only be searched for by the indirect methods discussed here and are therefore of prime interest, any detector which can study dark matter with α_H as small as 0.1 can exclude the bulk of the phase space currently available to MSSM dark matter candidates.

In the end we can just estimate the neutralino-nucleon cross section by dimensional analysis which gives $(G_F m_N^2)^2 / m_Z^2$. This also follows from (12) as m_H is of order m_Z

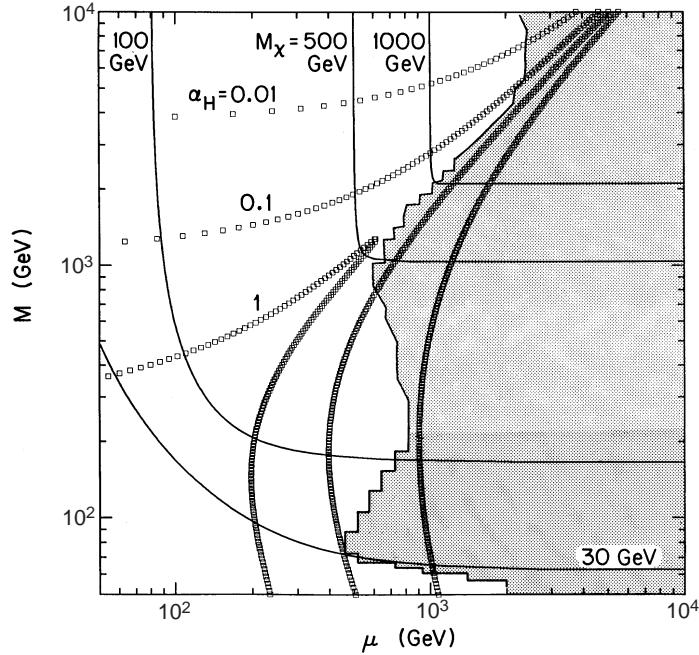


Fig. 4. Contours in the M, μ plane of constant $\alpha_{H_2} = 1.0, 0.1, 0.01$ (boxes) and constant neutralino mass $M_\chi = 30, 100, 500$ and 1000 GeV (solid). The shaded region is excluded by cosmological considerations.

in the MSSM. We obtain for the solar capture cross section

$$\Sigma_{\text{sun}} = n\sigma = \frac{M_{\text{sun}}}{m_N} \sigma(\chi N) = [1.2 \times 10^{57}] [10^{-41} \text{ cm}^2]. \quad (13)$$

Step 3: Capture rate N_{cap} of neutralinos by the sun

N_{cap} is determined by the neutralino flux (10) and the sun's capture cross section (13) obtained in the first 2 steps

$$N_{\text{cap}} = \phi_\chi \Sigma_{\text{sun}} = 3 \times 10^{20} \text{ s}^{-1}. \quad (14)$$

Step 4: Number of solar neutrinos of neutralino origin

One can check that the sun comes to a steady state where capture and annihilation of neutralinos are in equilibrium. For a 500 GeV neutralino the dominant annihilation rate is into weak bosons; each produces muon-neutrinos with a leptonic branching ratio which is roughly 10%:

$$\chi \bar{\chi} \rightarrow WW \rightarrow \mu \nu_\mu. \quad (15)$$

Therefore, as we get 2 W 's for each capture, the number of neutrinos generated in the sun is

$$N_\nu = \frac{1}{5} N_{\text{cap}} \quad (16)$$

and the corresponding neutrino flux at Earth is given by

$$\phi_\nu = \frac{N_\nu}{4\pi d^2} = 2 \times 10^{-8} \text{ cm}^{-2} \text{s}^{-1}, \quad (17)$$

where the distance d is 1 astronomical unit.

Step 5: Event rate in a high energy neutrino telescope

It is evident that this flux is small enough to require the use of large volumes of natural water or ice as a ν_μ interaction volume. The secondary muons produced in the interaction provide the experimental signature of the neutrinos in the underground detector; see Fig. 2. Optical modules view the water or ice target and detect the muon by the Cherenkov light emitted as it traverses the detector. By mapping the Cherenkov cone the solar origin of the neutrino can be established, at least for the higher energies where muon and neutrino directions are approximately aligned. The number of muons observed in a detector of a given area is

$$N = \text{area} \int dE \frac{dN_\nu}{dE} P_{\nu \rightarrow \mu}. \quad (18)$$

The quantity $P_{\nu \rightarrow \mu}$ represents the combined probabilities that a “solar” neutrino interacts in the volume viewed by the optical modules and that the muon, produced in the interaction, has a sufficient range to reach the detector. It depends on the particle density of the target, the neutrino interaction cross section and the range of the muon, therefore

$$P_{\nu \rightarrow \mu} = \rho_{\text{H}_2\text{O}} \sigma_{\nu \rightarrow \mu}(E) R_\mu. \quad (19)$$

Evaluating Eq. (19) only involves standard particle physics.

For (15) the W -energy is approximately m_χ and the neutrino energy half that by 2-body kinematics. The energy of the detected muon is given by

$$E_\mu \simeq \frac{1}{2} E_\nu \simeq \frac{1}{4} m_\chi. \quad (20)$$

where we used the fact that, in this energy range, roughly half of the neutrino energy is transferred to the muon. Simple estimates of the neutrino interaction cross section and the muon range can be obtained as follows

$$\sigma_{\nu \rightarrow \mu} = 10^{-38} \text{ cm}^2 \frac{E_\nu}{\text{GeV}} = 2.5 \times 10^{-36} \text{ cm}^2 \quad (21)$$

and

$$R_\mu = 5 \text{ m} \frac{E_\mu}{\text{GeV}} = 625 \text{ m}, \quad (22)$$

which is the distance covered by a muon given that it loses 2 MeV for each gram of matter traversed. We have now collected all the information to compute the number of events in a detector of area 10^4 m^2 , typical for those presently under construction. For the neutrino flux given by (17) we obtain

$$\# \text{ events/year} = \text{area} \times \phi_\nu \times \rho_{\text{H}_2\text{O}} \times \sigma_{\nu \rightarrow \mu} \times R_\mu \simeq 10. \quad (23)$$

Ten 125 GeV muons from the direction of the sun! It is a pretty safe bet that such a signal will not be drowned by whatever real world experimental problems dilute this naive estimate.

The above exercise is just meant to illustrate that present high energy neutrino telescopes compete with present and future accelerator experiments in the search for supersymmetry. Especially for heavier neutralinos the technique is powerful because underground high energy neutrino detectors have been optimized to be sensitive in the energy region where the neutrino interaction cross section and the range of the muon are large; notice the E -factors in (21), (22). Also, for high energy neutrinos the muon and neutrino are nicely aligned along a direction pointing back to the sun with good angular resolution. Direct searches will have to deliver detectors reaching better than 0.05 events/kg day sensitivity to compete.⁹

In many places we made assumptions that lead to an underestimate of the signal. We neglected, for instance, squark exchange contributions in (13) and neglected other decay channels contributing neutrinos in (16). We did not include the signal from annihilation of neutralinos trapped in the center of the Earth.¹⁰ We did, on the other hand, assume that α_H is unity while in some corners of SUSY-space the value is 2 orders of magnitude smaller; see Fig 4. Therefore the natural scale of the complete SUSY detector is two orders of magnitude larger than the 10^4 m^2 area of present detectors, i.e. 1 km^2 . This is the size next-generation neutrino telescopes already under discussion.¹¹ Such an instrument can be built with the number of phototubes of the SNO experiment in Canada and the budget of the Superkamiokande experiment in Japan. We will return to this further on.

4. Now for those who do not trust back-of-the-envelope

Above estimates can, of course, be done rigorously. This is tedious and straightforward. Our main conclusions are corroborated by the results of such a calculation shown in Fig. 5 which exhibits, as a function of the neutralino mass, the detector area required to observe one event per year. The two branches in this and the following figures correspond to the two solutions for a fixed neutralino mass; see Fig. 4. Various annihilation thresholds are clearly visible, most noticeable is the threshold associated with the W, Z mass near 100 GeV. The graphs confirm that, realistically, a detector of km-scale is required to study the full neutralino mass range. It is clear from Fig. 5, however, that even detectors of more modest size can radically improve on accelerator results.^{12,13} Neutralinos of 1 TeV mass are observable in a detector of area a few times 10^3 m^2 . The energy of the produced neutrinos is typically “a fraction” of the neutralino mass, e.g. 1/2 for neutralino annihilation into a W followed by a leptonic $e\nu$ decay. For lower masses the event rates are small because the detection efficiency for low energy neutrinos is reduced. This mass range has, however, already been excluded by accelerator experiments. For very high masses the number density of neutralinos, and therefore the event rate, becomes small. This is not a problem

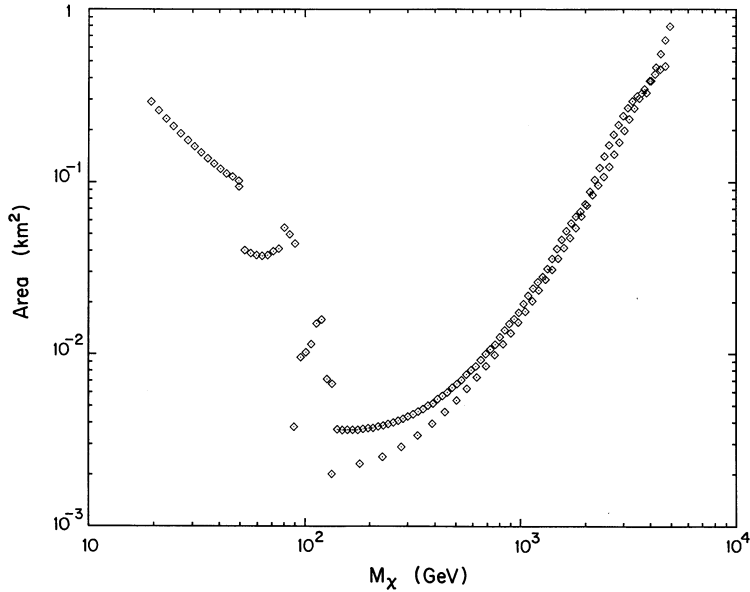


Fig. 5. As a function of the neutrino mass we show the telescope size required to be sensitive at the one event per year level. We fix $\tan \beta = 2$, $\alpha_{H_2} = 0.1$. The two branches correspond to the two solutions for fixed α_{H_2} .

as problematically large masses are excluded by theoretical arguments as previously discussed.

The same results are shown in Fig. 6 a as contours in the M, μ plane which denote the neutrino detection area required for observation of 1 event per year. Clearly the 10^5 m^2 contour covers the parameter space. The problematic large μ, M_2 -region does not represent a problem as its parameters lead to values of the matter density Ω exceeding unity as shown in the accompanying Fig. 6 b.

Clearly a realistic evaluation of the reach of an underground detector requires more than counting events per year. Realistic simulations of statistics and systematics must be done. Also a more complete mapping of the MSSM parameter space is required. For those interested we refer to reference 8.

5. High Energy Neutrino Telescopes

High-energy neutrino telescopes are multi-purpose instruments which can make contributions to astronomy, astrophysics and particle physics. It is intriguing that all of these missions, including the search for dark matter discussed here, point to the necessity of building 1 km^3 detectors.¹¹ We close with a discussion of the possibility of building a 1 km scale neutrino detector based on the experience gained in designing the instruments now under construction, specifically AMANDA, Baikal, DUMAND and NESTOR which we will briefly review.¹⁴ One can confidently predict that such a telescope can be constructed at a reasonable cost, e.g. a cost similar to

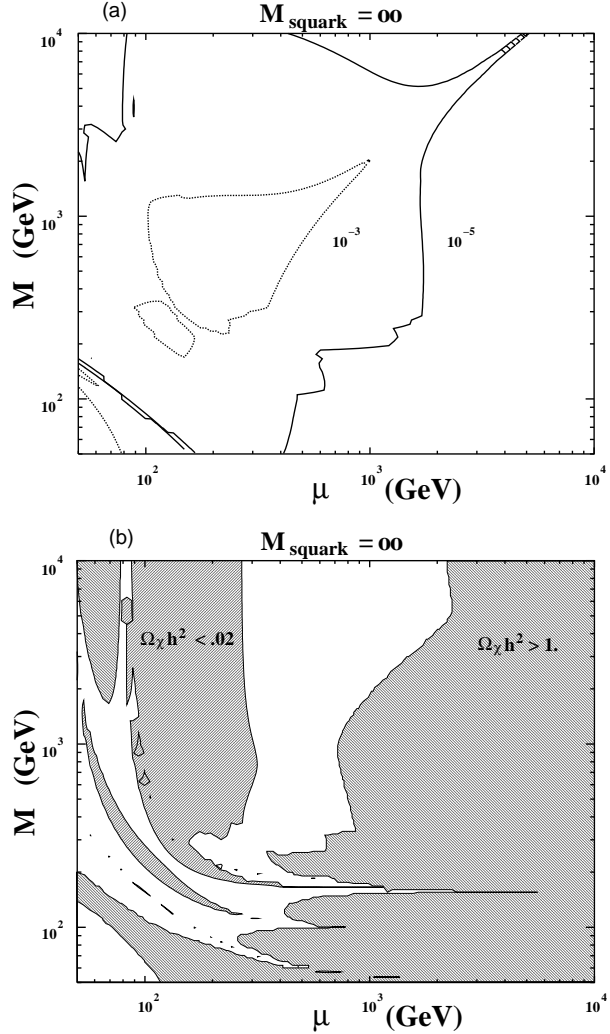


Fig. 6. In the M_2, μ plane for $M_{\tilde{q}} = \infty$, (a) contours of constant detection rate (events $\text{m}^{-2} \text{yr}^{-1}$) and (b) regions of $\Omega_\chi h^2 > 1$ and $\Omega_\chi h^2 < 0.02$ which are ruled out by cosmological considerations.

Superkamiokande,¹⁵ to which it is complimentary in the sense that its volume is over four orders of magnitude larger while its threshold is in the GeV, rather than the MeV range. The threshold is in the 2–10 GeV energy range for AMANDA and is about 10 GeV for DUMAND. Relative to a 1 km scale detector, the experiments under construction are only “few” percent prototypes. Yet, using natural water or ice as a detection medium, these neutrino detectors can be deployed at roughly 1% of the cost of conventional accelerator-based neutrino detectors which use shielding and some variety of tracking chambers. It is thus not hard to believe that the Cherenkov detectors can be extended to a larger scale at reasonable cost.

Detectors presently under construction have a nominal effective area of 10^4 m^2 . Baikal has been operating 18 optical modules for almost one year and the South Pole

AMANDA experiment started operating 4 strings with 20 optical modules each in January 94. The first generation telescopes will consist of roughly 200 optical modules (OM) sensing the Cherenkov light of cosmic muons. The experimental advantages and challenges are different for each experiment and, in this sense, they nicely complement one another. Briefly,

- DUMAND will be positioned under 4.5 km of ocean water, below most biological activity and well shielded from cosmic ray muon backgrounds. One nuisance of the ocean is the background light resulting from radioactive decays, mostly K^{40} , plus some bioluminescence, yielding an OM noise rate of 50–100 kHz. Deep ocean water is, on the other hand, fantastically clear, with an attenuation length of order 40 m in the blue. The deep ocean is a difficult location for access and service, not at all like a laboratory experiment. Detection equipment must be built to high reliability standards, and the data must be transmitted to the shore station for processing. It has required years to develop the necessary technology and learn to work in an environment foreign to high-energy physics experimentation, but hopefully this will be accomplished satisfactorily.
- AMANDA is operating in deep clear ice. The ice provides a convenient mechanical support for the detector. The immediate advantage is that all electronics can be positioned at the surface. Only the optical modules are deployed into the deep ice. Polar ice is a sterile medium with a concentration of radioactive elements reduced by more than 10^{-4} compared to sea or lake water. The low background results in an improved sensitivity which allows for the detection of high energy muons with very simple trigger schemes which are implemented by off-the-shelf electronics. Being positioned under only 1 km of ice it is operating in a cosmic ray muon background which is over 100 times larger than DUMAND. The challenge is to reject the down-going muon background relative to the up-coming neutrino-induced muons by a factor larger than 10^6 . The group claims to have met this challenge with an up/down rejection which is at present superior to that of the deep detectors. The task is, of course, facilitated by the low background noise. The polar environment is difficult as well, with restricted access and one shot deployment of photomultiplier strings. The technology has, however, been satisfactorily demonstrated with the deployment of the first 4 strings. It is now clear that the hot water drilling technique can be used to deploy OM's larger than the 8 inch photomultiplier tubes now used to any depth in the 3 km deep ice cover.
- NESTOR is similar to DUMAND, being placed in the deep ocean (the Mediterranean), except for two critical differences. Half of its optical modules point up, half down. The angular response of the detector is being tuned to be much more isotropic than either AMANDA or DUMAND, which will give it advantages in, for instance, the study of neutrino oscillations. Secondly, NESTOR will have

a higher density of photocathode (in some substantial volume) than the other detectors, and will be able to make local coincidences on lower energy events, even perhaps down to the supernova energy range (tens of MeV).

- BAIKAL shares the shallow depth with AMANDA, and has half its optical modules pointing up like NESTOR. It is in a lake with 1.4 km bottom, so it cannot expand downwards and will have to grow horizontally. Optical backgrounds similar in magnitude to ocean water have been discovered in Lake Baikal. The Baikal group has been operating for one year an array with 18 Quasar photomultiplier (a Russian-made 15 inch tube) units in April 1993, and may well count the first neutrinos in a natural water Cherenkov detector.
- Other detectors have been proposed for near surface lakes or ponds (e.g. GRANDE, LENA, NET, PAN and the Blue Lake Project), but at this time none are in construction.¹⁴ These detectors all would have the great advantage of accessibility and ability for dual use as extensive air shower detectors, but suffer from the 10^{10} – 10^{11} down-to-up ratio of muons, and face great civil engineering costs (for water systems and light-tight containers). Even if any of these are built it would seem that the costs may be too large to contemplate a full-km scale detector.

In summary, there are four major experiments proceeding with construction, each of which have different strengths and face different challenges. For the construction of a 1 km scale detector one can imagine any of the above detectors being the basic building block for the ultimate 1 km³ telescope. The present AMANDA design, for example, consists of 9 strings on a 30 meter radius circle with a string at the center (referred to as a 1 + 9 configuration). Each string contains 20 OMs separated by 12 m. Imagine AMANDA “supermodules” which are obtained by extending the basic string length (and module count per string) by a factor of 4.5. Supermodules would then consist of 1 + 9 strings with, on each string, 90 OMs separated by 12 meters for a length of 1080 meters. A 1 km scale detector then might consist of a 1 + 7 configuration of supermodules, with the 7 supermodules distributed on a circle of radius 540 meters, and have a total of about 7200 phototubes. Such a detector can be operated in a dual mode:

- it obviously consists of 4.5×8 of the presently planned AMANDA array modules, leading to an effective area of ~ 0.75 km². Importantly, the characteristics of the detector, including threshold, are the same as those of the original AMANDA array module.
- the 1 + 7 Supermodule configuration, looked at as a whole, instruments with OMs a 1 km³ cylinder with a diameter and height of 1080 m. High-energy muons will be superbly reconstructed as they can produce triggers in 2 or more of the modules spaced by large distance. Reaching more than one supermodule

requires 100 GeV energy to cross 500 m. For a 1 km deep detector the threshold for downgoing muons is thus raised from 200 to 300 GeV. We note that this is the energy for which a neutrino telescope has optimal sensitivity to a typical E^{-2} source (background falls with threshold energy, and until about 1 TeV little signal is lost).

Alternate methods to reach the 1 km scale have been discussed by Learned and Roberts.¹⁶

How realistic are the construction costs for such a detector? AMANDA's strings cost \$150,000 including deployment. By naive scaling the final cost of the postulated $1 + 7$ array of supermodules is of order \$50 million and still below that of Superkamiokande (with $11,200 \times 20$ inch photomultiplier tubes in a 40 m diameter by 40 m high stainless steel tank in a deep mine). It is clear that the naive estimate makes several approximations over- and underestimating the actual cost.

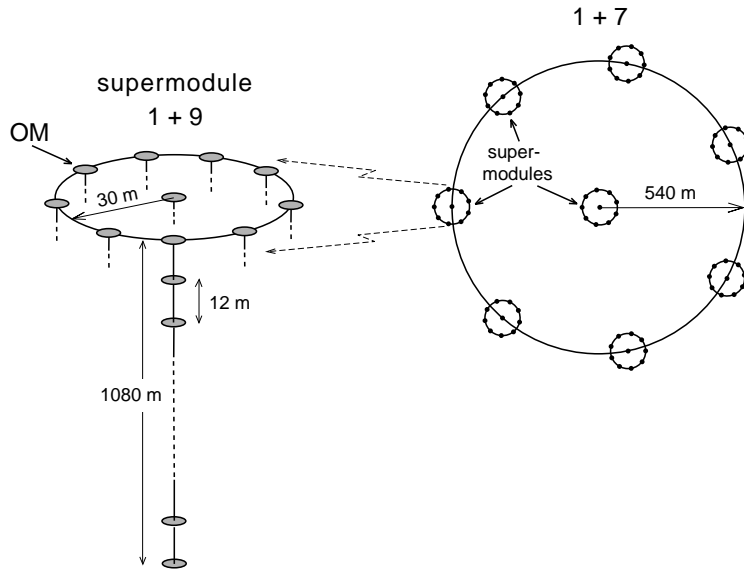


Fig. 7

At the 1 km² size it seems inescapable that supersymmetry will be found or, alternatively, will be forced to “escape” in rather special regions of its vast parameter space. The appeal of this beautiful theoretical idea would be diminished.

Acknowledgements

We would like to thank Steve Barwick, Manuel Drees, Concha Gonzalez-Garcia and Marc Kamionkowski for useful conversations. This research was supported in part by the U.S. Department of Energy under Contracts No. DE-FG02-91ER40626 and No. DE-AC02-76ER00881, in part by the Texas Research National Commission under Grant No. RGFY9173, and in part by the University of Wisconsin Research Committee with funds granted by the Wisconsin Alumni Research Foundation.

References

1. J. R. Primack, B. Sadoulet, and D. Seckel, Ann. Rev. Nucl. Part. Sci. **B38** (1988) 751.
2. V. S. Berezinsky, *Proc. of the Fourth International Symposium on Neutrino Telescopes*, Venice (1992), ed. by M. Baldo-Ceolin.
3. H. E. Haber and G. L. Kane, Phys. Rep. **117**, 75 (1985).
4. M. Drees and M. M. Nojiri, Phys. Rev. **D47**, 376 (1993).
5. For a recent review, see T. K. Gaisser *et al.*, *The Astrophysics and Particle Physics of High Energy Cosmic Radiation*, National Research Council Research Briefing, Washington (1994).
6. For updated calculations and references, see G. Jungman and M. Kamionkowski, Princeton Preprint IASSNS-HEP-93/54, 1993.
7. M. Kamionkowski and M. S. Turner, Phys. Rev. **D43**, 1774 (1991) and references therein.
8. F. Halzen, M. Kamionkowski, and T. Stelzer, Phys. Rev. **D45**, 4439 (1992).
9. A. Bottino *et al.* Mod. Phys. Lett. A **7**, 733 (1992).
10. A. Gould, Astrophys. J. **321**, 571 (1987); Astrophys. J. **368**, 610 (1991); Astrophys. J. in press (1991).
11. F. Halzen and J.G. Learned, *Proc. of the Fifth International Symposium on Neutrino Telescopes*, Venice (1993), ed. by M. Baldo-Ceolin.
12. M. Mori *et al.*, KEK Preprint 91-62; N. Sato *et al.*, Phys. Rev. **D44**, 2220 (1991).
13. IMB Collaboration: J. M. LoSecco *et al.*, Phys. Lett. **B188**, 388 (1987); R. Svoboda *et al.*, Astrophys. J. **315**, 420 (1987).
14. See recent reports on these experiments in the following reference, and a critical summary of the various projects in J. G. Learned, *Proceedings of the European Cosmic Ray Symposium*, Geneva, Switzerland, July 1992, ed. by P. Grieder and B. Pattison, Nucl. Phys. B (1993); see also presentations in *Proceedings of the High Energy Neutrino Astrophysics Workshop*, ed. by V. J. Stenger, J. G. Learned, S. Pakvasa, and X. Tata, World Scientific, Singapore (1992).
15. Y. Suzuki, *Proceedings of the 3rd International Workshop on Neutrino Telescopes*, Venice, March 1992, ed. by M. Baldo-Ceolin, Venice (1992).
16. J. G. Learned and A. Roberts, *Proceedings of the 23rd International Cosmic Ray Conference*, Calgary, Canada (1993).

This figure "fig1-1.png" is available in "png" format from:

<http://arxiv.org/ps/hep-ph/9404252v1>

This figure "fig2-1.png" is available in "png" format from:

<http://arxiv.org/ps/hep-ph/9404252v1>

This figure "fig1-2.png" is available in "png" format from:

<http://arxiv.org/ps/hep-ph/9404252v1>

This figure "fig2-2.png" is available in "png" format from:

<http://arxiv.org/ps/hep-ph/9404252v1>

This figure "fig1-3.png" is available in "png" format from:

<http://arxiv.org/ps/hep-ph/9404252v1>

This figure "fig1-4.png" is available in "png" format from:

<http://arxiv.org/ps/hep-ph/9404252v1>

This figure "fig1-5.png" is available in "png" format from:

<http://arxiv.org/ps/hep-ph/9404252v1>